

LED/Area Array CCD Multiformat Film Scanner for Digital Photofinishing

Mark E. Shafer and Joel D. DeCaro
Eastman Kodak Company
Rochester, NY USA

Abstract

Several fully digital minilabs for the retail photofinishing market have been recently introduced. These systems greatly expand the products and services that retail photofinishers now can offer to consumers. Inputs and outputs are no longer just “analog” — film, and prints. Photofinishers can now offer better quality prints and enlargements, in a wider range of formats, as well as providing access to digital images on floppy disks, CDs, and via the Internet. Additionally, they can offer these services from a wider range of inputs — from film and prints, as well as from digital cameras, images from disk, and the Internet.

Kodak has developed a film-scanner for such a system. This scanner accepts both color negative and reversal film types, in 35 mm and Advanced Photo System-formats. All film handling is automated, for speed and labor savings, as is typical for this photofinishing market segment. Images are scanned at resolutions up to 2000 x 3000 pixels (“16Base”), and speeds exceeding 1000 frames/hour. Speed and resolution are programmable, and can be traded off to produce 1000 x 1500 pixel (“4Base”) images at 1900 frames/hour, for example.

One common paradigm for the architecture of such a film scanner utilizes a linear (or trilinear) charge-coupled device (CCD), and a tungsten illumination source. This scanner is unusual, in that a full-frame area CCD sensor architecture is combined with LED-based illumination. This paper will discuss the physics behind this choice, as well as the advantages that result.

Physics of the Measured Signal and its Quality

The basic components of a scanner, which influence the signal measured for each pixel across the film’s surface, are illustrated in Fig. 1, below.¹ Light from an illumination system of spectral radiance $L(\lambda)$, impinges on the film object. That light passing through the pixel area, A_o , at the film is modulated by the film’s spectral transmittance, $\tau(\lambda)$, in accordance with the image contained therein. The solid angle of light leaving the film, Ω_o , and collected by the optical system, is imaged onto a detector of area A_I .

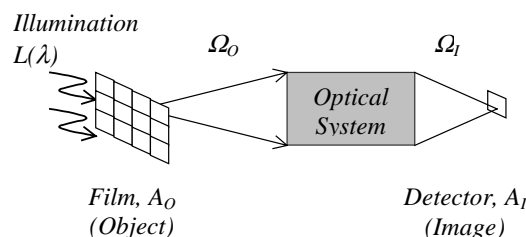


Figure 1.

Because optical extent, $A\Omega$, is constant,²

$$A_o\Omega_o = A_I\Omega_I \quad (1)$$

the radiant flux may be computed in either the film or detector plane. The product of the radiance, area, and solid angle ($LA\Omega$) gives the amount of radiant flux. So the radiant flux available for detection and measurement, taking into account the spectral characteristics of the film and source, is

$$\int \tau(\lambda)L(\lambda)A_o\Omega_o d\lambda \quad (2)$$

Optical detectors serve to convert this radiant flux from a flow of photons to a flow of electrons, via the photoelectric effect.³ This conversion efficiency is not 100%; it varies with detector types and wavelength (among other things), and is termed the quantum efficiency, ϵ_q . And so the flow of electrons is given by

$$\int \epsilon_q(\lambda)\frac{\lambda}{hc}\tau(\lambda)L(\lambda)A_o\Omega_o d\lambda \quad (3)$$

where h is Plank’s constant, c is the speed of light, and the term λ/hc serves to convert flux from units of power to photons per second. If this flow of electrons is integrated for a period of time, T , then a finite number of electrons will have been collected.

$$N_e = T \int \epsilon_q(\lambda)\frac{\lambda}{hc}\tau(\lambda)L(\lambda)A_o\Omega_o d\lambda \quad (4)$$

The film transmittance, τ , is proportional to the above, and is computed by normalizing to 100% transmittance, that is, an "open gate" measurement where $t(\lambda) = 1$. An alternate way to express this would be

$$N_{e^-} = tN_{OGe^-} \quad (5)$$

where N_{OGe^-} represents the number of electrons for the "open gate" condition.

One measure of the signal's quality is the signal-to-noise ratio, or SNR. Shottky's theorem⁴ states that the RMS noise is equal to the square root of the number of electrons.

$$\sigma_{N_{e^-}} = \sqrt{N_{e^-}} \quad (6)$$

And so the SNR becomes

$$\begin{aligned} SNR &= \frac{N_{e^-}}{\sigma_{N_{e^-}}} = \sqrt{N_{e^-}} \\ &= \sqrt{T \int \epsilon_q(\lambda) \frac{\lambda}{hc} \tau(\lambda) L(\lambda) A_o \Omega_o d\lambda} \end{aligned} \quad (7)$$

To be sure, at low signal levels, the "shot" noise component described above falls below so-called "dark" noise components, which are independent of signal level. *Very roughly*, this may occur around 1000 e^- , or 30 e^- RMS, and depends heavily on the sensor and measurement electronics.

The Trade-off between Radiometry, Speed, Resolution, and Noise Requirements

From the foregoing discussion, it is evident that the integration time, detector quantum efficiency, illumination system radiance, pixel area, and solid angle of collection all contribute to determining the SNR. For a given detector (with some quantum efficiency), one can specify any three of the remaining parameters, and solve for the fourth.

Further, it is instructive to identify the requirements from more commonly used terms related to these parameters, that is, in terms of speed, resolution and noise.⁵ Illumination requirements can then be distilled from these. Analyzing the problem this way allows scanners across a wide range of applications and speeds to be compared. This concept can also be used to assess the relative merits of various scanning architectural approaches.

In the following sections, the relationship of these parameters to the more common attributes of speed, resolution and noise will be discussed. Values will be established that are pertinent to a minilab photofinishing scanning application.

Speed

Scanning speed is often specified in confusing ways. What is essential is to reduce the requirement to the signal integration time, T .

A typical minilab photofinishing speed requirement is ~40 "orders per hour", where an order consists of about 25 image frames from one filmstrip. Taking away about 15

seconds per order, for operator film handling, leaves 75 seconds per 25 frames, or about 3.0 seconds frame-to-frame cycle time. Frame advance requires ~0.5 second. The amount of time left for signal integration depends upon the detector architecture chosen. With a linear CCD, the integration and readout occur simultaneously. However, 3000 lines must be processed in 2.5 seconds; hence the integration time per line would be 833 μ seconds. With a full-frame area CCD, however, the signal integration (or exposure) and readout of the device must be performed serially. Still, the integration time can be more than 2 orders of magnitude higher than in the linear CCD case.

Resolution

Resolution is perhaps an unfortunate choice of words. Scanner "resolution" is often quoted with values that simply indicate the scanner sampling pitch; that is, a "600 dots-per-inch" (dpi) scanner. The important quantity to specify is the modulation transfer function (MTF), which is a measure of the spatial frequency response of the system. MTF is affected by both the aperture area at the object plane, A_o , and by the collection solid angle, Ω_o , of the optical system. What follows is a simple model of this,⁶ so that reasonable parameter values for the photofinishing scanner example can be established.

For rectangular apertures, the MTF along one axis is given by

$$MTF_{Aperture} = \frac{\sin(\pi h \nu)}{(\pi h \nu)} \quad (8)$$

where h is the width along that edge of the aperture, and ν is the spatial frequency.

The optical system is often a lens. Assuming small-angle approximations, the collection solid angle is related to the lens effective, or "working" $f/\#$ at the object by

$$\Omega_o = \frac{\pi}{(2f/\#)^2} \quad (9)$$

An upper bound for the lens MTF is given by its diffraction-limited performance,

$$MTF_{Lens} = \frac{2}{\pi} \left[\cos^{-1}(x) - x\sqrt{1-x^2} \right]$$

where

$$x = f/\# \lambda \nu \quad (10)$$

A lens is seldom perfectly diffraction limited. However, as a rough model, it is useful to adjust the working $f/\#$ such that the diffraction-limited MTF is approximately equivalent to the real lens being considered.

A film-scanner digitizing 2000 x 3000 pixels from 35 mm format film (about 23.0 x 34.5 mm) would have a sampling frequency of about 87 cyc/mm; the sampling pitch would be about 11.5 μ m. This would also be the dimension of the aperture at the film plane, assuming the detector has 100% fill-factor. An $f/13$ diffraction-limited lens would

possess a reasonable MTF; that this is so is shown in Fig. 2 (where 550 nm wavelength light is assumed).

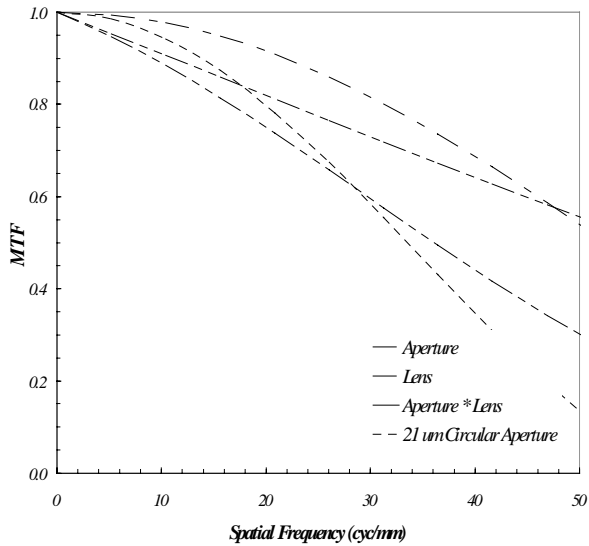


Figure 2.

In Fig. 2, the combined aperture and lens MTF has about 35% modulation at the 43.5 cycles/mm half-sampling frequency. Aliasing would normally be a concern with this approach, but it should be remembered that the film and camera taking-lens each have an MTF. An average f/8 camera lens might have ~50% modulation around 50 cycles/mm. The same is roughly true for films, of course depending on film speed.⁷ Hence, the net MTF would be on the order of 10%, and the aliasing potential is reduced to an acceptable level.

Some comments on depth of field are warranted, as the choice of working f/# affects this, and so affects the mechanical film gate design. An f/13 system might have about $\pm 175 \mu\text{m}$ depth of focus. Holding film flat around the frame edges of cut filmstrips, especially in the presence of film curl, can be a challenge.

A “faster” lens (lower working f/#) will obviously improve the light gathering capability (i.e., increase Ω_0). However, if the film gate and optical system mechanical designs are not carefully addressed, it is unlikely the MTF will be improved. Conversely, a “slower” lens and/or a sloppy mechanical design can degrade the MTF to the point that scanning at 87 cycles/mm is no longer warranted.

Noise

Noise performance is likely an aspect of the scanner that is the least well specified. More often than not, scanner descriptions or comparisons concentrate on the “scan time” and “dpi”, and say little or nothing about noise. Occasionally, the “dynamic range” is quoted, but it is usually unclear as to what is being measured and reported. (There is even discrepancy among CCD vendors on this definition.)

Still, it is important to define the metric, as well as to have a basis for the requirement. Having done this, one can

recognize its impact on speed, resolution, and the required illumination system radiance.

One basis for setting this requirement might be to compare the noise of the scanner to the “noise” of the film being scanned. Film “noise” is subjectively observed as “graininess” in an image. One objective measure is referred to as granularity.⁸ In this measure, a film sample is diffusely illuminated, while a small circular scanning aperture is moved across the films’ surface. Both the average density, and the RMS density are measured. The data are sometimes reported only at a single density. (Obviously, the SNR of such a system is designed to be substantially lower than the film noise being measured!) Density is related to the films’ transmittance via

$$D = -\log_{10}(\tau) \quad (11)$$

More complete data from one such measurement, using a 48 μm circular aperture, is shown in Fig. 3 below. The data shown is typical of a 200-speed color negative film, and is plotted as density, and RMS density, both as a function of film log (exposure). The dark gray data point on each curve shows approximately where a “normally” exposed 20% gray patch would lie. The exposure from a diffuse 100% white patch is 5 times this exposure, or 0.7 log (exposure) above that of the gray patch. A 4-stop overexposed scene (which will still produce an excellent image from film) moves these points 8x, or 1.2 log (exposure). Thus, the white point of a 4-stop over-exposed scene will lie about 0.7 + 1.2, or about 1.9 log (exposure) above the indicated point — in other words, right around the 0.0 log (exposure) point at the right-hand edge of this figure.

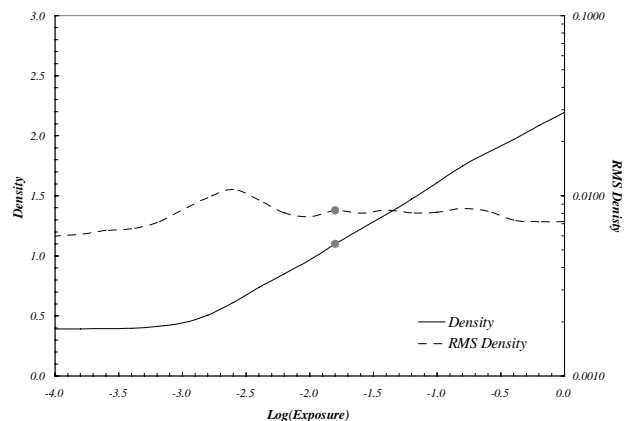


Figure 3.

Two things must be done with this data, so that it can be compared with scanner noise.

First, this data is based upon a 48 μm circular aperture, which is not the same as the aperture and lens previously described for the scanner. In Fig. 2, along with the scanner’s combined aperture and lens MTF curve, is a 2nd curve showing the MTF of a 21 μm circular aperture. As the spatial bandwidth of this curve is roughly the same as that developed for the scanner, the scanner is said to have a

scanning aperture roughly equivalent to that of a 21 μm circular aperture.

Selwyn's law⁵ states that the variance of the granularity is proportional to the aperture area; alternatively, the RMS value is proportional to the aperture diameter. This relationship begins to fail as the film grain dimensions approach that of the aperture. In effect, the film grain noise power spectrum is being approximated as a constant over the spatial bandwidth considered. As the film grain is smaller than this,⁵ Selwyn's law holds, so the 48 μm data can be simply scaled (by 48/21 or ~ 2.3) to the 21 μm condition.

The second thing that must be done with this data is to plot it versus the signal measured by the scanner — that is, the RMS granularity should be plotted versus density. Figure 4 shows the result of re-scaling granularity data to a 21 μm effective aperture, and plotting this versus density.

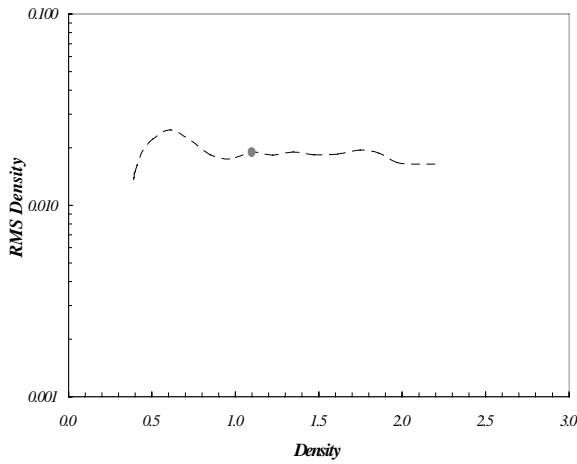


Figure 4.

Now this must be compared to scanner noise. Taking the first derivative of equation (11), the noise in density space can be related to the noise in transmittance space,

$$\sigma_{Density} = \frac{1}{\ln(10)} \frac{\sigma_{\tau}}{\tau}. \quad (12)$$

Note the second term on the RHS is essentially the “noise-to-signal” ratio. Referring back to the “shot” noise component of equations (4) and (7), equation (12) can be rewritten as

$$\sigma_{Density} = \frac{1}{\ln(10)} \frac{1}{\sqrt{\pi N_{OGe^-}}} = \frac{1}{\ln(10)} \frac{1}{\sqrt{10^{-D} N_{OGe^-}}} \quad (13)$$

By observation, when plotted on a semi-log plot, this component will exhibit a slope of $1/2$ — see Fig. 5, below.

There is also a “dark” noise component, which is independent of signal level. This arises from the average dark current within the detector itself, as well as from other sources, output amplifiers, and A-to-D converters for example. If we define dynamic range (DR) as the ratio of

the peak signal to the RMS dark noise, σ_{τ} , becomes $1/DR$. Thus, the dark noise component in density space is

$$\sigma_{Density} = \frac{1}{\ln(10)} \frac{1}{10^{-D} DR} \quad (14)$$

On the same type plot, this component has a slope of 1. The total scanner noise is the root-sum-square of these two components, as they are uncorrelated. The density at which the scanner noise transitions from being shot- to dark-noise limited occurs at

$$D_{x-over} = -\log_{10} \left(\frac{N_{OGe^-}}{DR^2} \right). \quad (15)$$

For 100Ke⁻ and 4000:1 DR, this occurs at a density of 2.20, also shown in Fig. 5.

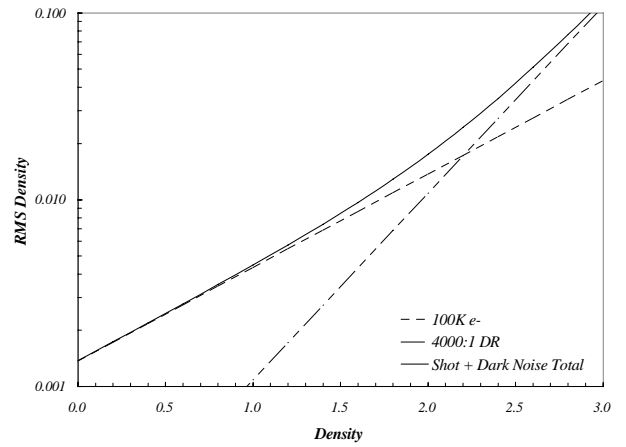


Figure 5.

An additional improvement can be made. Color negative film has an orange cast to the unexposed film base. This is referred to as the minimum density (D_{min}). Quantitatively, this can be seen in figure 3, at $-4.0 \log$ (exposure) — the D_{min} for this layer is about 0.4. The detector will never see signals below a density of 0.4 (or above a transmittance of 0.40). In optical terms, this is a transmission loss, and amounts to wasted dynamic range.

If the system exposure is adjusted to compensate for this lost light (through longer integration times or increased radiance), by an amount equal to $10^{D_{min}}$, both the DR and the N_{OGe^-} are effectively increased by this amount. The noise equations are modified as follows. The shot noise component becomes

$$\sigma_{Density} = \frac{1}{\ln(10)} \frac{1}{\sqrt{10^{-(D-D_{min})} N_{OGe^-}}} \quad (16)$$

The dark noise component becomes

$$\sigma_{Density} = \frac{1}{\ln(10)} \frac{1}{10^{-(D-D_{min})} DR} \quad (17)$$

and the density at which the scanner noise transitions from being shot- to dark-noise limited increases to

$$D_{x-over} = D_{min} - \log_{10} \left(\frac{N_{0Ge^-}}{DR^2} \right) \quad (18)$$

In effect, every component is right-shifted along the density axis by D-min.

Plots are shown in Figs. 6, 7, and 8 below, juxtaposing the film noise with the scanner noise, for the red, green and blue layers respectively.

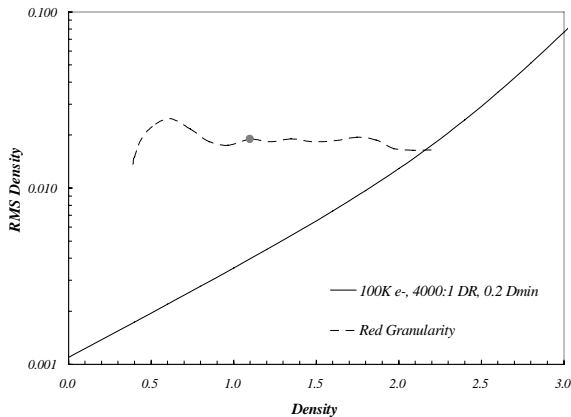


Figure 6.

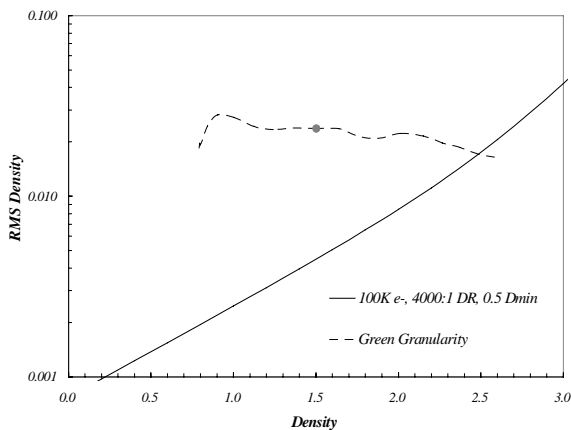


Figure 7.

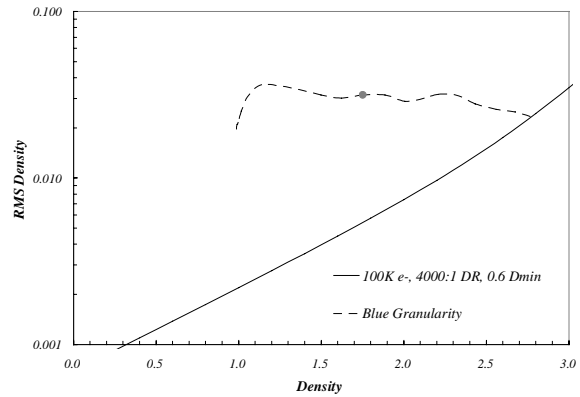


Figure 8.

As can be seen from these plots, the noise performance resulting from the combination of 100Ke⁻, 4000:1 dynamic range, and increasing the exposure to accommodate D-min values of (0.2, 0.5, 0.6), easily exceeds the noise performance of this 200-speed film, up to about 4-stops of overexposure.

This particular film has base density values even higher than those specified above. If the D-min exposure adjustments were made to match this film, a larger range of overexposure could be handled.

Comparison of Linear, Area CCD Approaches

In addition to the previously identified parameters, the red, green and blue spectral bandwidths and peaks should be set – this analysis used (30, 30, 45) nm bandwidths located at (470, 550, 700) nm respectively.⁹

Additionally, it is well known in the photographic trade that diffuse illumination is used to suppress scratches and other surface imperfections. Each of the approaches below assumes the illumination output is Lambertian; the power output is calculated as $\pi LA_{illumination}$, the area of illumination.

Trilinear CCD Approach.

The tri-linear CCD scanner must expose and readout ~3000 RGB lines in 2.5 seconds, and position the next frame in 0.5 seconds. The integration time is 833 μ sec. The sensor readout is 2.5 MHz for each RGB channel. The quantum efficiency values are approximate for a pinned-photodiode sensor. The illumination area is assumed to be 2.6 cm x 0.3 cm.

Full-frame area CCD approach.

This area CCD approach will sequentially expose and readout each color. Readout can be completed in about 0.7 seconds, using a 10 MHz data rate. Also note, the 0.5 second film advance can be completed during the last color channel's readout. Hence, 2.1 of the 3.0 seconds frame time are utilized just for readout. The remaining 0.9 seconds may be equally split, for 0.3 seconds integration time, per color. The quantum efficiency values are approximate for sensor of this type. The illumination area is assumed to be 2.6 cm x 3.8 cm.

The results are summarized in tables 1 and 2, below. The shaded rows indicate the areas of difference between the approaches.

Table 1. The trilinear CCD system values

	B	G	R	
N_{e-}	1.00E+05	1.00E+05	1.00E+05	e-
ϵ_q	0.40	0.50	0.60	
D-min	0.60	0.50	0.20	
N_{photons}	9.95E+05	6.32E+05	2.64E+05	photons
h	6.60E-34			J*sec
c	3.00E+08			m/sec
λ	4.70E-07	5.50E-07	7.00E-07	m
$T_{\text{integration}}$	8.33E-04			sec
Power	5.03E-10	2.73E-10	8.97E-11	W
A_{obj}	1.32E-06			cm ²
f/#	1.30E+01			
Ω_{obj}	4.65E-03			sr
$\Delta\lambda$	30	30	45	nm
L	8.19E-02	4.45E-02	1.46E-02	W/cm ² *sr
$L(\lambda)$	2.73E-03	1.48E-03	3.24E-04	W/cm ² *sr*nm
A_{illum}	0.78			cm ²
P	2.01E-01	1.09E-01	3.58E-02	W
$P(\lambda)$	6.69E-03	3.63E-03	7.95E-04	W/nm

Table 2. The area CCD system values

	B	G	R	
N_{e-}	1.00E+05	1.00E+05	1.00E+05	e-
ϵ_q	0.2	0.35	0.4	
D-min	0.6	0.5	0.2	
N_{photons}	1.99E+06	9.04E+05	3.96E+05	photons
h	6.60E-34			J*sec
c	3.00E+08			m/sec
λ	4.70E-07	5.50E-07	7.00E-07	m
$T_{\text{integration}}$	3.00E-01			sec
Power	2.80E-12	1.08E-12	3.74E-13	W
A_{obj}	1.32E-06			cm ²
f/#	13.00			
Ω_{obj}	4.65E-03			sr
$\Delta\lambda$	30	30	45	nm
L	4.55E-04	1.76E-04	6.08E-05	W/cm ² *sr
$L(\lambda)$	1.52E-05	5.88E-06	1.35E-06	W/cm ² *sr*nm
A_{illum}	9.9			cm ²
P	1.41E-02	5.49E-03	1.89E-03	W
$P(\lambda)$	4.71E-04	1.83E-04	4.20E-05	W/nm

Discussion and Conclusions

The area approach gathers light from more pixels simultaneously (by a factor of 3×10^3), so the integration

time can be longer, and radiance lower. The full-frame area approach is less efficient due to serial operation. Still, the area system is advantaged by ~200 times. In Tables 1 and 2, the spectral radiance values are approximately 150, 250, and 240 times lower.

Optical power from the illuminator is also much lower for the area case. Notice that while the combined pixel area for the linear scanner is $3 \times 2000 \times 1.32E-6$, or $7.8E-3 \text{ cm}^2$, the illuminated area is 0.78 cm^2 . This over-illumination is necessary for scratch suppression, and represents a ~90% loss. The loss from over-illumination in the area case is ~20%. In Tables 1 and 2, the RGB power is approximately 15, 20, and 19 times lower.

The magnitude of the spectral radiance is a good indicator of what type of light source must be used.¹ The linear scanner requires $2.7E-3 \text{ W/cm}^2\text{*sr*nm}$ spectral radiance at 470 nm. A 3200K tungsten filament produces about 10 to $15E-3 \text{ W/cm}^2\text{*sr*nm}$ - about 4 times more. Losses in making a diffuse, linear illumination slit of are on this order. The lamp power would be about 100 to 200 W. In stark comparison, the radiance and power for the area scanner indicate that light-emitting diodes (LEDs) can be used. With the advent of gallium nitride blue and green LEDs, having 1.0 to $2.0E-3 \text{ W}$ output, such a scanner is now a reality.

LEDs bring many additional advantages. They can be easily modulated to adjust exposure time. The illumination system requires no moving filter wheels or shutters. The area CCD requires no mechanical shutter. This operation is ideally suited to a full-frame CCD architecture.

Area CCD costs are higher. However, historical technology trend data indicate this disadvantage will continue to shrink. This, combined with the added system cost of the linear approach, makes an LED / full frame area CCD approach extremely attractive.

References

1. J. R. Milch, Imaging Processes and Materials, Van Nostrand Reinhold, New York NY, 1992, pg. 292.
2. W. J. Smith, Modern Optical Engineering, McGraw-Hill, New York NY, 1966, pg. 183.
3. R. T. Weidner and R. L. Sells, Elementary Modern Physics, Allyn and Bacon Inc., 1973, pg. 106.
4. R. E. Ziemer and W. H. Tranter, Principles of Communications, Houghton Mifflin Co., Boston MA, 1976, pg. 472.
5. J. C. Dainty and R. Shaw, Image Science, Academic Press Inc., New York NY, 1974, pgs. 24, 38, 137, 220.
6. J. W. Goodman, Introduction to Fourier Optics, McGraw Hill Book Co., 1968, pg. 101.
7. L. Stroebel, J. Compton, I. Current and R. Zakia, Photographic Materials and Processes, Focal Press - Butterworth Publishers, Stoneham MA, 1986, pg. 406.
8. R. W. G. Hunt, The Reproduction of Color, Fountain Press, England, 1987, pg. 342.
9. W. C. Kress and J. P. Alessi, The Influence of Film, Paper and Printer Spectral Characteristics on Photofinishing Performance, *J. App. Photogr. Eng.*, vol. 9 no. 2, pg. 58 (1983).